

Unlocking Potential Capacity Benefits of Electric Vehicles (EVs) with Adaptive Cruise Control (ACC)

Servet Lapardhaja¹, Kemal Ulas Yagantekin², Mingyuan Yang¹, Tasnim Anika Majumder², Xingan (David) Kan^{2,*}, Mohamed Badhrudeen Mohamed Rawoof²

¹Institute of Transportation Studies, Department of Civil and Environmental Engineering, University of California, Berkeley, CA 94720-1720

²Department of Civil, Environmental, and Geomatics Engineering, Florida Atlantic University, Boca Raton, FL 33431-0991

*Corresponding author; E-mail: kanx@fau.edu

Unlocking Potential Capacity Benefits of Electric Vehicles (EVs) with Adaptive Cruise Control (ACC)

ABSTRACT

Today's mainstream vehicles are partially automated via Adaptive Cruise Control (ACC) that relies on on-board sensors to automatically adjust speed to maintain a safe following distance. Contrary to expectations for automated vehicles, ACC may reduce capacity at bottlenecks because its delayed response and limited initial acceleration during queue discharge could increase the average headway. Fortunately, EV's unique powertrain characteristics such as instantaneous torque and regenerative braking could allow ACC to adopt shorter headways and accelerate more swiftly to maintain shorter headways during queue discharge, therefore reverse the negative impact on capacity. This has been verified in a series of field experiments, which demonstrate that EVs with ACC could potentially achieve a capacity as high as 2,931 veh/hr/lane in steady-state conditions, and it can be sustained in non-steady-state conditions where speeds fluctuate and queues form.

Keywords: Adaptive Cruise Control (ACC), Electric Vehicle (EV), vehicle automation, capacity, field test

Word Count: 7986 words

1. Introduction

Advancements in vehicle automation and driver assistance have presented new opportunities to transportation researchers and practitioners as they promise to be an alternative solution to reduce traffic congestion. While full automation may not yet be production ready, partial automation has become ubiquitous today. Using on-board sensors such as radar, most of the new vehicles sold today can automatically adjust the speed and maintain a safe following distance via an advanced driver assistance systems (ADAS) feature known as adaptive cruise control (ACC). ACC on today's mainstream vehicles can operate at both high and low speeds, including in stop-and-go conditions.

ACC adoption and market penetration have been increasing over time since its introduction and will eventually require traffic engineers and planners to re-evaluate their assumptions about traffic flow characteristics in the coming years. Meanwhile, many researchers have paid significant attention to the traffic flow impact of ACC, primarily to ACC equipped vehicles powered by internal combustion engines (ICE). Specifically, many have conducted field experiments and developed models to show that the longitudinal car following behavior of ACC is string unstable, in which minor speed fluctuations amplify into major disturbances further upstream (Gunter et al. 2019; Knoop et al. 2019; Makridis, Mattas, and Ciuffo 2019; Gunter et al. 2020; Ciuffo et al. 2021; Li et al. 2021; Makridis et al. 2021; M. Wang et al. 2018). In addition, contrary to the expectation that automated vehicles could mitigate congestion, ICE powered vehicles equipped with ACC may reduce roadway capacity and increase congestion, and this has been investigated through simulation and field experiments (Vander Werf et al. 2002; James et al. 2019; Chon Kan, Lapardhaja, and Kan 2021; Lapardhaja et al. 2021; Shang and Stern 2021; Chon Kan, Murshed, and Kan 2022). Specifically, ACC could increase the

average headway at queue discharge because the limited initial power and torque generated by ICE leads to delayed response during initial acceleration. This could reduce capacity, as suggested by field experiments (Chon Kan, Lapardhaja, and Kan 2021; Chon Kan, Murshed, and Kan 2022). To capture these field observations, many have developed microscopic level car following models (Milanés and Shladover 2014; He et al. 2022; Shang, Rosenblad, and Stern 2022; Yang et al. 2022) and macroscopic level models such as the fundamental diagram (Shi and Li 2021; Li et al. 2022) for ACC equipped vehicles. Others have investigated the interaction between ACC and human drivers (Gong et al. 2022). Overall, a plethora of research findings on the traffic flow impact of ACC have been negative or do not report significant benefits (James et al. 2019; Vander Werf et al. 2002; Shang and Stern 2021; Shladover, Su, and Lu 2012; Alkim, Bootsma, and Hoogendoorn 2007; Mattas et al. 2018).

Unfortunately, these research efforts have only concentrated on vehicles equipped with ICE and at most hybrid electric powertrain, and there is still a lack of knowledge about how low-level automated vehicles such as ACC equipped vehicles will affect capacity when paired with fully electric powertrain, which has significantly different power delivery, acceleration, and braking characteristics. Interestingly, electrification of vehicle powertrain has become increasingly ubiquitous and mainstream, and the combination of fully electric vehicles (EVs) with ADAS could present new opportunities that have not yet been discovered. This is an important area that deserves significant attention, especially considering the ever-increasing popularity and market penetration of EVs as stricter emissions regulations will incentivize greater EV adoption in the near future.

1.1. Background: EV powertrain characteristics

The combination of EVs and ADAS features such as ACC cannot be overlooked when modeling

traffic flow because the unique powertrain characteristics of fully EVs could present significant opportunities to improve capacity and reduce congestion. ICE gradually increases its torque output as the engine speed increases. Since power is the product of torque and engine speed, higher power output on ICE would only be attainable after reaching higher engine speeds, and ICE yields low to moderate acceleration prior to peak acceleration at the highest engine speed. But realistically, human drivers seldom operate at high engine speeds but rather at low to medium engine speeds (3500 revolutions per minute or lower) to maintain driver comfort, reasonable fuel economy, and long-term reliability of the vehicle powertrain. This is because ICE cannot deliver both efficiency and performance at the same time, and modern transmissions paired with ICE are typically designed to avoid operating at larger gear ratios and higher engine speeds unless there is a strong demand for acceleration. Similarly, ADAS features such as ACC are designed to behave alike and an ACC equipped vehicle that is paired with ICE could not generate significant power and acceleration during normal operation conditions (at medium to low engine speeds, as designed by the ACC control algorithm). Conversely, EVs produce very high maximum torque almost instantaneously at relatively low engine speeds, when accelerating from both higher and lower speeds. Revisiting the concept that power is the product of torque and engine speed, EVs could produce relatively higher power at lower ranges of engine speeds as illustrated in Figure 1. As a result, the unique powertrain characteristics of EVs mean that EVs yield an immediate higher acceleration for a broad range of speeds under normal operating conditions¹, at low to medium engine speeds, which is the typical operation condition for ADAS

¹ During the field experiments in this study, it was evident that the brisk acceleration of EVs equipped with ACC provided a comfortable and smooth ride for passengers, without any jarring sensations.

features such as ACC. This enhanced performance at a broad speed range also translates to higher energy efficiency in EVs when compared to ICE vehicles (Fiori et al. 2019), particularly in congested traffic. Moreover, the electric motors of EVs apply regenerative braking immediately upon releasing the throttle, and the regenerative braking alone could yield an instantaneous deceleration of as much as 2.5 m/s^2 on mainstream EVs. If the mechanical brakes were applied in addition to the regenerative braking effect from simply releasing the throttle, EVs could easily apply a deceleration of 5.0 m/s^2 without much delay. Combining the instantaneous torque with the strong braking performance from electric motor's regenerative braking, EVs with ACC could potentially adopt shorter headways and accelerate more swiftly to maintain shorter headways when speeds fluctuate and during queue discharge, thereby improve capacity and reverse the previously mentioned negative impact of ACC. While it appears promising, this claim must be validated by observations from field experiments. Unfortunately, none have specifically addressed the impact of pairing ACC with EVs unique powertrain characteristics on roadway capacity.

[Figure 1 here]

This study intends to conduct field tests to quantify the potential impact of EVs with ACC on capacity. The field tests provide a novel and comprehensive set of trajectory level car following data that encompasses most of the traffic conditions, the data could then be used to

¹ During the field tests, the maximum acceleration rate did not exceed 2.5 m/s^2 while average deceleration rate was about 3.4 m/s^2 . Those rates fall within the recommended ranges for operation of transportation facilities and geometric design (AASHTO 2018; ITE 2009). The main difference is that those acceleration and deceleration values were more attainable and can be sustained longer over a wide range of speeds.

develop and calibrate models at the microscopic level, and the corresponding models could be integrated into simulation for prospective analyses on the traffic flow impact of EVs with ADAS and serve as an analysis tool for developing traffic operations and control strategies for future scenarios with higher EV adoption. This comprehensive dataset captures steady-state traffic conditions as well as non-steady-state conditions in which queues form and speed fluctuations and disturbances are present; these speed fluctuations and disturbances may represent real world traffic features such as ingress and egress of traffic from on-ramps and off-ramps, turning movements, etc. and low-speed queues that form near bottlenecks. Microscopic level trajectory data are collected using high precision GPS from a series of carefully designed car-following experiments using EVs with ACC to capture a leader and follower interaction and important parameters such as minimum headway and spacing, and speed and acceleration profiles. These experiments replicate real world conditions when vehicles travel in steady-state conditions with constant headways, reduce speeds when queues form, and accelerate during queue discharge at and near bottlenecks. This study discusses the analysis of GPS data from the field to determine the potential impact of ACC on capacity in a variety of traffic conditions.

In the following section, the experiment setup and characteristics are presented. Next, the experimental data is analysed and the implication on capacity is discussed. Finally, conclusions are drawn and recommendations for future work are discussed. Lastly, in the Appendix, a description of the dataset is provided.

2. Research Approach: Field Experiments

Conducting experiments through field observations is the most reliable method for this research because there are currently no established simulation tools that could accurately model the

behavior of EVs equipped with ACC². Ideally, installing cameras or detectors on roadways typically yields the most accurate measurement for flow, capacity, density, and mean speeds. However, this method cannot yield any meaningful and viable results in today's traffic stream because there is currently a very low market penetration of ACC-equipped EVs. Instead, this study will prospectively assess the impact of ACC-equipped EVs on capacity by examining GPS data collected from carefully designed car following experiments in controlled environments using two test vehicles: a leading vehicle as the point of reference, and a following vehicle that is an EV equipped with ACC. Furthermore, the empirical data could serve as benchmark data to develop and calibrate car following models that are used as inputs for microscopic simulation, which could scale-up the two-vehicle car following experiment to analyses of larger traffic streams. Specifically, an ICE vehicle (2021 Toyota Camry) with a 3,310 lb. curb weight and maximum power output of 203 horsepower at 6,600 rpm from a 2.5-liter naturally aspirated engine was used as the leading vehicle in the field experiments. For the following vehicle, we selected a mainstream EV (2022 Hyundai IONIQ 5) with a curb weight of 4,414 lbs. and the powertrain delivers 225 horsepower and 258 lb.-ft. of torque. These selections are intended to ensure consistency with previous experiments (Chon Kan, Lapardhaja, and Kan 2021; Chon Kan, Murshed, and Kan 2022) by maintaining a similar a weight-to-power ratio. We assume that the EVs selected in this field test could potentially represent a large portion of mainstream ACC-equipped EVs on the road in the near future. Moreover, recent studies demonstrate that the variations between different ACC systems from several manufacturers are not significant (Makridis, Mattas, and Ciuffo 2019). Consequently, we anticipate that the findings in this

² Currently, there are no validated car following models designed to accurately capture the behavior of ACC-equipped EVs using real-world data.

experiment can be generalized in the near future, as mainstream EVs with ACC become more prevalent³. The ACC system of EVs used in this study is functional in full-speed range and has four different following gap settings (short, medium, long, and extra-long) for the driver to select from, which can generate a wide range of the headways and spacings.

In addition to testing the Hyundai IONIQ 5, the field test included two other electric vehicles (EVs) from different manufacturers – the 2022 Tesla Model 3 and the 2023 Polestar 2, under the same scenarios for comparison. The Tesla Model 3 has a curb weight of 3,686 pounds, and its powertrain generates 221 horsepower and 302 lb-ft of torque. The Polestar 2, on the other hand, has a curb weight of 4,400 pounds and an output of 231 horsepower and 243 lb-ft of torque from its powertrain. Although the power to weight ratio of the Tesla Model 3 is inconsistent and much more favorable compared with the other EVs tested, the Tesla Model 3 was selected to be inclusive of the popular options in today's EV market. EV models from other manufacturers were not attainable or available at the time of field experiments. An ICE vehicle (2022 Toyota Corolla) with a 2,910 lb. curb weight and maximum power output of 139 horsepower at 6,000 rpm from a 1.8-liter naturally aspirated engine was used as the leading vehicle in the field experiments involving the Tesla Model 3 and Polestar 2 as the following vehicles. To avoid bias, the vehicles used in the field tests were consumer-grade vehicles obtained from car rental agencies and dealerships, identical to the vehicles available to ordinary consumers and not vehicles specially prepared by the vehicle manufacturers.

Trajectory data from both the leading and following vehicles were collected using one of the most advanced GPS devices known as Racebox. Racebox offers a remarkably high 25 Hz

³ As EV market shares grow and more EV models become available further investigation on their distinct behavior needs to be conducted.

frequency and an excellent 10 cm accuracy, for collecting position data including variables such as latitude, longitude, and altitude every 0.04 seconds and compute cumulative distance traveled, speed and acceleration. The GPS coordinates obtained could also be used to determine spacing and headway between adjacent vehicles.

To ensure the synchronization of the timestamps from both GPS devices and minimize errors, a carefully designed pre-experiment procedure was implemented. This involved performing a synchronized deceleration of both vehicles from a predetermined speed, followed by a frame-by-frame analysis of accompanying video footage. This allowed for the precise alignment of the data sets, thereby reducing errors associated with timestamp offset.

2.1. Car following experiments

Initially, both vehicles were aligned in a single lane with an (initial) spacing (front bumper to front bumper) of $l + \Delta$ of each other, where l is the leading vehicle length and Δ is a fixed distance to prevent collisions between the leading vehicle's rear bumper and the following vehicle's front bumper. Then, the two vehicles sequentially began to accelerate manually up to a pre-defined free-flow speed, and we conducted experiments for four different free-flow speeds: 96 km/hr, 88 km/hr, 72 km/hr, and 56 km/hr. To avoid safety hazards and unnecessary interruption to nearby traffic at the test site, speeds above sustained free flow speeds above 96 km/hr and below 56 km/hr were not considered. After reaching the pre-defined free-flow speed, the driver of the following vehicle (EV) activated the ACC with the desired speed set the same as the free-flow speed, or 8 km/hr (5 mph) or 16 km/hr (10 mph) than the free-flow speed, depending on the experimental trial that is performed. The driver of the leading vehicle activated the cruise control and the remained at the free-flow speed. To minimize the spacing between the

vehicles, the following vehicle's driver manually accelerated slightly beyond the pre-defined free-flow speed. Afterward, the driver re-activated ACC, allowing it to automatically adjust the spacing relative to the leading vehicle. This stabilization process is intended to replicate the equilibrium condition at capacity, in which vehicles enter the roadway from various locations and adjust their headways and spacings and eventually reach the minimum allowable spacing (and headway) to be sustained for an extended period and distance, therefore achieving the maximum sustained flow (and capacity). At this point, there have not been interruptions due to merging, changes in speed limit, or other potential disruptions that could cause a bottleneck, reduce speed, form queues, or even potentially diminish capacity. A set of the effective timestamps of both vehicles was chosen after this stabilization process is completed at time t ; for example, their stable cruising speed (after stabilization) is identical at 96 km/hr as shown in Figure 2. Beyond the time t , the cumulative distance traveled and spacing can be calculated to estimate the minimum headway and maximum flow (at capacity) under steady-state condition.

[Figure 2 here]

The field experiments are also intended to study the car following behaviors of ACC-equipped EVs beyond steady-state conditions; for example, at bottlenecks where vehicles approach the back of the queue and accelerate during queue discharge. To replicate slight speed fluctuations and larger speed fluctuations observed at bottlenecks, the driver of the leading vehicle applied normal decelerations manually to a congested speed that is lower than the free-flow speed. This deceleration can represent disruption from a sudden change in speed limit, merging vehicles from on-ramps, diverging vehicles at and near off-ramps, etc. Such a scenario can lead to a bottleneck and allow queues to form. Then, both vehicles returned to their initial free-flow speed after staying at a lower speed for 10 seconds or more if conditions allow. The

driver of the leading vehicle accelerated manually under normal acceleration while the following vehicle accelerated via ACC. This process enables the replication of queue discharge that occurs downstream of a bottleneck. For each free-flow speed, the cycle of deceleration and acceleration is repeated for various congested speeds lower than the free-flow speed. Table 1 illustrates the tested free-flow speeds with their corresponding lower speeds. Figure 3 displays an example of the speed profile tested with 88 km/hr free-flow speed and various congested speeds in the speed fluctuations. Similar procedures were applied to experiments using other free-flow speeds shown in Table 1. In total, 136 repetitions were performed for all gap settings, encompassing various free-flow speeds and speed fluctuations with vehicles having the same desired speed.

[Table 1 here]

[Figure 3 here]

To complement the aforementioned experiments, additional repetitions were conducted to study the effects of the ACC's behavior when the maximum desired speed of the following vehicle exceeds the leading vehicle's free-flow speed. Two scenarios were examined, one where the maximum desired speed of the following vehicle was +8 km/hr higher and another where it was +16 km/hr higher. Overall, an additional 136 repetitions were performed for all gap settings, covering a wide range of free-flow speeds and speed fluctuations with the following vehicles having +8 and +16 km/hr higher maximum desired speeds (68 trials for each desired speed combination).

2.2. Test sites and Data Analysis

Field experiments were conducted on isolated portions of rural public roads in Dixon, California, on approximately 10-km stretches of Pendrick, Robben, and Sikes Rds. The remote locations and

lack of interference from other road users allowed us to reproduce various traffic conditions efficiently throughout the data collection process. Robben Rd. was primarily used while Pedrick Rd. and Sikes Rd. were alternate locations in case the conditions were less ideal on Robben Rd.

Vehicle trajectories were constructed using the position data (longitude and latitude) generated from each Racebox GPS unit every 0.04 seconds in the field experiments. These vehicle trajectories were used to extract joint estimates of spacing and headway between the leading and following vehicle.

3. Results and Discussion

Field experiments demonstrate that EVs with ACC can achieve considerably shorter headways, reaching as low as 1.23 seconds at constant speeds in steady-state conditions. This could potentially yield higher capacities of up to 2,931 veh/hr⁴, compared to ICE vehicles with ACC. This finding is consistent with initial attempts to quantify the headways adopted by ACC controllers at constant speeds in steady-state conditions (Li et al. 2022). This is a result of EV's instantaneous regenerative braking that allows EVs to safely follow the preceding vehicles more closely at higher speeds. Table 2 summarizes the minimum headways and time gaps under steady-state conditions for ACC-equipped EVs (IONIQ 5) across a range of free-flow speeds, spanning from 56 km/hr to 96 km/hr. Similar to previous studies on ICE vehicles equipped with ACC (Chon Kan, Lapardhaja, and Kan 2021; Chon Kan, Murshed, and Kan 2022), it is observed that the minimum headway for EVs increases as the selected ACC gap setting transitions from short to medium to long, and to extra-long. This same pattern is also evident when examining the

⁴ More investigations through simulations to account for discretionary lane changes, heterogenous desired speeds and other conditions are needed to investigate the impact on capacity.

time gaps. However, it is noteworthy that, when considering time gaps, the speed-related differences within the same gap setting are not particularly significant. The speed-related variations can be attributed to ACC's proprietary car following algorithm that accounts for the gap with respect to the leading vehicle, instead of headway that includes the vehicle length. Similar gaps at different speeds could lead to slight variations in headways at different speeds when the vehicle length is accounted for.

[Table 2 here]

For ICE vehicles with ACC, a similar experiment by (Chon Kan, Lapardhaja, and Kan 2021; Chon Kan, Murshed, and Kan 2022) observed that the minimum headways are typically 1.89 seconds on average and nearly 3 seconds if the longest gap was selected. Compared with the values shown in Table 2, EVs with ACC have the potential to provide higher capacity due to shorter headways regardless of the speed and the preferred ACC gap selected by the driver. For example, Table 2 shows that ACC equipped EVs could potentially achieve minimum headways of 1.23, 1.50, and 1.77 seconds while traveling at 96 km/hr in steady-state conditions with ACC set for short, medium, and long gaps, respectively. On the other end, EVs with ACC could potentially yield minimum headways of 1.27, 1.60, and 1.84 seconds while traveling at 56 km/hr in steady-state conditions with ACC set for short, medium, and long gaps, respectively.

In addition to the minimum headways established by the ACC controllers, the field experiments demonstrated that there was relatively low variability in the observed minimum headways: Figure 4 illustrates the distribution of the minimum headway for EVs (IONIQ 5) with ACC at free-flow speeds of 96 km/hr, 88 km/hr, 72 km/hr, and 56 km/hr in steady-state conditions. This could potentially yield more reliable and consistent capacities in real world traffic. Notably, this lower variability in minimum headways for EVs with ACC starkly contrasts

with the field experiments involving ACC-equipped ICE vehicles (Chon Kan, Lapardhaja, and Kan 2021; Chon Kan, Murshed, and Kan 2022) and their findings, which revealed significant variability in the minimum headway values, particularly for medium and long gap settings, despite similar experimental conditions being for both EVs and ICE-powered vehicles.

[Figure 4 here]

Unlike ACC-equipped ICE vehicles, these shorter headways adopted by ACC equipped EVs can be sustained beyond the ideal steady-state conditions. The exceptional powertrain characteristics of fully electric vehicles (EVs) enabled responsive deceleration using regenerative braking when approaching the back of queue when a leading vehicle is decelerating, and most importantly, the instantaneous peak torque allowed for nearly immediate acceleration once the leading vehicle began accelerating during queue discharge. This sustained the shorter headways adopted by EVs with ACC and entails that the potentially higher capacities could be sustained even in non-steady-state conditions, where speeds fluctuate when queues form and dissipate at bottlenecks. Table 3 illustrates the sustained short headways, demonstrated by the minimal deviation in headways regardless of the ACC gap setting and the extent of the speed fluctuation, which may result from queue formation at freeway entrances and exits or near turning maneuvers. Previous research on ACC-equipped ICE vehicles showed that headways increased by approximately 1 second for the short gap and 1.3 seconds and 1.6 seconds for the medium and long gap, respectively (Chon Kan, Lapardhaja, and Kan 2021), due to the ACC controller's delayed response and sluggish acceleration during car following and queue discharge. Of course, this can be attributed to ICE's progressive torque power delivery with initial lower output that leads to initially unresponsive acceleration. In contrast, Table 3 demonstrates that ACC-equipped EVs exhibit minimal headway change, with all cases falling below 0.1 seconds. As a result,

minimum headways and maximum flows remain consistent with the steady-state minimum headways depicted in Table 2. Notably, even when both vehicles have the same desired speed (a desired speed difference of 0), the headway change remains negligible, thereby preserving the minimum headway. Most of all, this is true regardless of how the following vehicle's desired speed was chosen; ACC in EVs maintains constant headway as speeds fluctuated.

[Table 3 here]

Figure 5 presents a time-space diagram for both the leading and following vehicles. As depicted in the plots, the ACC-equipped EV follower Hyundai IONIQ 5 regained its initial minimum headway following a speed fluctuation intended to simulate approaching back of queue and accelerating during queue discharge, which contrasts with the performance of conventional ACC-equipped ICE vehicles, as shown by Figure 6 obtained from earlier field experiments (Chon Kan, Lapardhaja, and Kan 2021). Figure 6 illustrates that ACC-equipped ICE vehicle exhibits a reaction delay (possibly from the ICE powertrain) and very gradual initial acceleration when returning to free-flow speeds (88 km/hr in this example) during queue discharge, all of which are findings from an earlier study as benchmark. This gradual acceleration corresponds to a rate of approximately 0.5 m/s^2 to 1.0 m/s^2 on a regular basis, which is a very leisurely increase in speed. In the end, the headway increases. EVs produce strong initial acceleration from the instantaneous peak torque, and as illustrated in Figure 5, the slope of the time-space diagram is steeper for EV's acceleration. In fact, careful examination of field data suggests that EVs can accelerate normally and smoothly at almost twice the rate (1.5 m/s^2 to 2.0 m/s^2).

[Figure 5 here]

[Figure 6 here]

Moreover, steep decrease in speed and strong deceleration can be found on the trajectories in Figure 5. This resembles the aggressive regenerative braking of EVs, and the better braking performance allows ACC-equipped EVs to safely follow the leading vehicle at shorter headways. Interestingly, shown in Figure 5, the aggressive regenerative braking applied by the following vehicle Hyundai IONIQ 5 ACC did not amplify the speed change from the 88 km/hr free-flow speed to the 40 km/hr congested speed in this example. This is certainly different from the example shown in Figure 6, where the ACC-equipped ICE vehicle amplified the speed change relative to the speed fluctuations undertaken by the leading vehicles.

Observations from both field tests and trajectories in Figures 5 and 6 revealed that ACC-equipped EVs immediately applied aggressive regenerative braking that enabled the follower to quickly reach and maintain its desired headway as leader began decelerating, whereas the limited braking capability resulted in the ACC-equipped ICE vehicle (follower) to decelerate for an extended period to speeds below that of the leading vehicle's final speed in the congested state (after the leader completed decelerating) to finally reach its desired headway, and ultimately amplifies speed change. This stark contrast could mean that ACC-equipped EVs may improve stability of traffic⁵, a vastly different outcome than the string unstable car following behavior of ACC-equipped ICE vehicles demonstrated in Figure 6 and confirmed by various prior experiments (Gunter et al. 2019; Knoop et al. 2019; Makridis, Mattas, and Ciuffo 2019; Gunter et al. 2020; Ciuffo et al. 2021; Li et al. 2021; Makridis et al. 2021).

⁵ Field tests with a larger platoon of vehicles and simulations (Zare et al. 2023) need to be conducted to examine whether ACC-equipped EVs improve string stability compared to ACC-equipped ICE vehicles.

Overall, we observed that the headway values are nearly identical for before and after speed fluctuations (i.e., disturbance) with a shorter headway than that of ACC-equipped ICE vehicles. This highlights the superior capability of the ACC-equipped EVs in maintaining nearly constant and steady headways in dynamic real world traffic conditions.

Furthermore, these field experiments suggest another interesting finding: setting higher desired speed does not affect the car following behavior. As ACC-equipped EV accelerates swiftly to follow the lead vehicle and maintain the minimum headway, it would not be possible to accelerate beyond the leading vehicle speed even if the ACC desired speed was set higher, due to the minimum spacing and headway constraint. Figure 7 shows the speed vs. time plots of an example scenario. As shown, setting ACC desired speeds 8 or 16 km/hr above the desired speed (free-flow speed) of the leading did not alter the car following trajectories, in comparison with the scenario shown in Figure 5. On the other hand, ACC-equipped ICE vehicles would accelerated beyond the speed of the leading vehicle to undergo a “catch-up” process before decelerating again to ensure that the minimum headway is maintained, shown in Figure 8 (Yang, Kan, and Yagantekin 2023).

[Figure 7 here]

[Figure 8 here]

As mentioned earlier, we conducted comparative tests using ACC equipped EVs from two other manufacturers, the Polestar 2 from a traditional but premium manufacturer Volvo and the Tesla Model 3 from an emerging vehicle manufacturer Tesla, using the same procedures and under similar conditions albeit with fewer repetitions. The observations obtained from testing the Polestar 2 mirrored those from the experiments using the Hyundai IONIQ 5, exhibiting similar minimum headways and sustained almost constant headways even in non-steady-state conditions

when queues are present. As depicted in Figure 9, the time-space diagram shows similar trajectories when decelerating while the Polestar 2 approaches the back of queue and when accelerating during queue discharge, though there appears to be a slight amplification of the speed change as opposed to the trajectories in Figure 5. However, the results for the Tesla Model 3 deviated from our expectations, as evidenced in Figure 7. Unlike the car following behavior of other ACC equipped EVs such as the Hyundai IONIQ 5 and Polestar 2, the Tesla Model 3 was unable to regain its initial minimum headway after a speed fluctuation, exhibiting characteristics similar to those of ACC-equipped ICE vehicles. This is reflected in the larger minimum headways and greater variability in minimum headways, leading to a substantial increase. Furthermore, a comparison with the time-space diagrams corresponding to the same experimental scenario for the ACC equipped ICE vehicle tested in (Chon Kan, Lapardhaja, and Kan 2021; Chon Kan, Murshed, and Kan 2022) show that the Tesla Model 3’s car following behavior is much similar to that of an ACC equipped ICE vehicle. It appears that the ACC equipped by Tesla does not utilize the advantages of EV powertrain, especially the instant peak torque that provides immediate acceleration during queue discharge, instead, the ACC equipped by Tesla gradually accelerates at a leisurely pace as the leading vehicle accelerates during queue dissipation. Similarly, the same “catch-up” process associated with ACC-equipped ICE vehicles that is shown in Figure 8 can be found in Figure 11, when the desired speed of the follower (Tesla Model 3) is set higher than that of the leader.

[Figure 9 here]

[Figure 10 here]

[Figure 11 here]

To shed light on the divergent behavior of Tesla, as compared to the other ACC-equipped EVs such as the Hyundai IONIQ 5 and Polestar 2, we delved into the distribution of accelerations and decelerations. As demonstrated in Figure 12, the analysis revealed that while in operation with ACC, Tesla Model 3 exhibits smoother acceleration and deceleration rates, with a higher distribution of lower acceleration rates and deceleration rates as compared to the Hyundai IONIQ 5 in the same set of experiments. This observation provides a crucial insight into the behavior of Tesla's ACC system, suggesting that its algorithm is configured to exhibit a more sluggish behavior akin to that of ACC-equipped ICE vehicles, despite its powertrain capabilities to be more responsive.

As an added note, the same string unstable behavior can be observed when examining Tesla Model 3's trajectory in ACC mode, shown in both Figure 10 and Figure 11. The speed change was amplified relative to the speed change underwent by the leading vehicle, same as the trajectories that correspond to ACC-equipped ICE vehicles, shown in Figures 6 and 8. Of course, this has broader implications for shockwaves and queue propagation that requires further analyses.

Finally, the field experiments also revealed that the ACC system equipped by Tesla cannot maintain constant headway even at constant speeds and in steady-state conditions, and this often led to inconsistent car following behavior that could render traffic flow modeling difficult and unreliable.

Nevertheless, this set of experiments provides very important initial insights on the potential benefits of electric powertrain to vehicle automation going forward. The data generated from these carefully planned experiments could be used to develop and validate microscopic level models for car following, which could be used as the underlying assumption in a scaled-up

simulation of macroscopic traffic. Ultimately, the true capacity benefit that EVs with automation could offer would be validated and affirmed given the appropriate models and simulation tools developed based on empirical observations.

[Figure 12 here]

4. Conclusion and Recommendation

Commercially available Adaptive Cruise Control (ACC) equipped vehicles have become increasingly prevalent on roads today. ACC is an Advanced Driver Assistance Feature (ADAS) that allows for partial automation by automatically adjusting speed and maintaining safe following distance using data collected from on-board sensors. Today's commercial ACC systems can operate in all speed ranges and are equipped on most new mainstream vehicles. The increasing adoption of fully electric vehicles (EVs) has brought new opportunities; EV's unique operating characteristics such as instantaneous torque and strong regenerative braking could improve capacity and mitigate congestion when EVs are paired with ACC.

Field experiments demonstrate that ACC equipped EVs can achieve minimum headways as short as 1.23 seconds at constant speeds in steady-state conditions. This could potentially lead to an improved capacity as high as 2,931 veh/hr/lane. Moreover, deviations from the steady-state conditions do not affect the minimum headway, as shown by an extensive set of field experiment with a wide range of speed fluctuations to simulate approaching back of the queue and queue discharge at and near disturbances and bottlenecks that may arise from ingress and egress at freeway on and off-ramps, turning movements, etc. Furthermore, EVs equipped with ACC could potentially not amplify speed changes further upstream, which could imply better stability of the traffic stream and less abrupt queue propagation. Overall, ACC-equipped EVs could outperform ICE vehicles with ACC, as well as human drivers, in terms of the potential capacity and

congestion reduction benefits. Interestingly, this only applies to the tested EVs from some manufacturers, whereas the tested EVs from other manufacturers such as Tesla deliver car following dynamics akin to an ICE vehicle with ACC⁶.

We recommend future experiments to capture the effect of lane change on ACC-quipped EV's car following behavior, as the receiving lane change car following behavior may be distinct from what had been observed in the car following experiments presented in this paper. In addition, future studies should conduct field tests in naturalistic environments where traffic conditions are more stochastic. Moreover, field tests should be conducted in mixed environments with a combination of both ICE vehicles and EVs, especially ICE vehicles following EVs to determine the potential impact of mixed traffic stream with vastly different powertrain characteristics. Finally, given the valuable data presented in this field study, future work should develop car following models unique to ACC-equipped EVs to capture the microscopic level car following behavior, and this would establish an important foundation for developing simulation platforms to perform prospective analyses at large scale. This would address many unknowns related to ACC-equipped EVs, examples include macroscopic models such as the fundamental diagram and the effectiveness of implementing dedicated lane for fully electric vehicles operating in ACC mode, and all of which will prepare future researchers and practitioners for new opportunities in traffic operations and management in the era of increasingly automated and electrified vehicles. Especially in the near term, when the market penetration of ACC-equipped EVs is relatively small and traffic engineers will need to rely heavily on effective traffic management strategies such as preferential lane treatment or dynamic tolls to fully take

⁶ As the Autopilot technology evolves and software updates change further investigation is required on the car following dynamics.

advantage of the capacity benefits offered by EVs equipped with ACC. Most of all, the effect of powertrain characteristics on traffic flow is often overlooked and this study will shed light on a new but very important perspective for traffic flow and operations in the coming years, as electrification of vehicle fleet becomes more common. This experimental work could also be expanded to test many variations of electric powertrain or motors, for example those with different nominal voltages. Finally, electric powertrain may also be a better fit for CACC-equipped vehicles because EVs could easily satisfy the immediate acceleration and braking demanded by CACC control design when vehicle platoons travel with very short headways. Although there have been many recent studies on the capacity, string stability, and energy consumption benefits of CACC (Yu, Hua, and Wang 2023; Liu, Lu, and Shladover 2020; Hung and Zhang 2022; W. Wang and Wu 2023; H. Wang et al. 2019; Liu, Lu, and Shladover 2019; Liu et al. 2018; Liu et al. 2021), none have specifically addressed the potential benefit of CACC equipped on EVs. Nevertheless, there has been recent empirical evidence demonstrating the implementation feasibility of CACC on all types of powertrains including electric powertrain (Flores et al. 2023). We suggest future work to investigate how electric powertrain uniquely impact or benefit CACC operations in terms of stability, capacity, and energy consumption.

Acknowledgments

This paper and the work described were sponsored by the National Science Foundation (NSF) under the Civil Infrastructure Systems (CIS) program, award number 2301446.

Declaration of Interest

The authors declare that they have no known competing financial interests or personal relationships that could have appeared to influence the work reported in this paper.

Data Availability

The car-following data collected can be found at <https://github.berkeley.edu/mingyuan-yang/MicroSimACC-EV>.

Author Contributions

Servet Lapardhaja: Methodology, Software, Validation, Formal analysis, Investigation, Data Curation, Writing - Original Draft, Writing - Review & Editing, Visualization. **Kemal Ulas Yagantekin:** Validation, Formal analysis, Investigation, Data Curation, Writing - Original Draft, Writing - Review & Editing, Visualization. **Mingyuan Yang:** Methodology, Software, Validation, Investigation, Data Curation, Writing - Review & Editing, Visualization. **Tasnim Anika Majumder:** Validation, Formal analysis, Investigation, Data Curation, Writing - Original Draft, Writing - Review & Editing, Visualization. **Xingan (David) Kan:** Conceptualization, Methodology, Validation, Investigation, Resources, Writing - Original Draft, Writing - Review & Editing, Supervision, Project administration, Funding acquisition. **Mohamed Badhrudeen Mohamed Rawoof:** Investigation, Data Curation.

References

AASHTO. 2018. *A Policy on Geometric Design of Highways and Streets*. <https://trid.trb.org/view/1552370>.

Alkim, Tom P, Gerben Bootsma, and Serge P Hoogendoorn. 2007. "Field Operational Test" the Assisted Driver". In *2007 IEEE Intelligent Vehicles Symposium*, 1198–1203. IEEE.

Chon Kan, Pablo, Servet Lapardhaja, and Xingan David Kan. 2021. "Field Experiments of Commercially Available Automated Vehicles on Freeways." In *Transportation Research Board 100th Annual Meeting*.

Chon Kan, Pablo, Md Imran Murshed, and Xingan David Kan. 2022. "Field Experiment on the Impact of Automated Vehicles on Arterial Capacity – Case Study of Adaptive Cruise Control." In *Transportation Research Board 101st Annual Meeting*.

Ciuffo, Biagio, Konstantinos Mattas, Michail Makridis, Giovanni Albano, Aikaterini Anesiadou, Yinglong He, Szilárd Josvai, Dimitris Komnos, Marton Pataki, and Sandor Vass. 2021. "Requiem on the Positive Effects of Commercial Adaptive Cruise Control on Motorway

Traffic and Recommendations for Future Automated Driving Systems.” *Transportation Research Part C: Emerging Technologies* 130. Elsevier: 103305.

Fiori, Chiara, Vincenzo Arcidiacono, Georgios Fontaras, Michail Makridis, Konstantinos Mattas, Vittorio Marzano, Christian Thiel, and Biagio Ciuffo. 2019. “The Effect of Electrified Mobility on the Relationship between Traffic Conditions and Energy Consumption.” *Transportation Research Part D: Transport and Environment* 67 (February): 275–290. doi:10.1016/j.trd.2018.11.018.

Flores, Carlos, John Spring, David Nelson, Simeon Iliev, and Xiao-Yun Lu. 2023. “Enabling Cooperative Adaptive Cruise Control on Strings of Vehicles with Heterogeneous Dynamics and Powertrains.” *Vehicle System Dynamics* 61 (1). Taylor & Francis: 128–149. doi:10.1080/00423114.2022.2042568.

Gong, Yaobang, Pablo Chon Kan, Servet Lapardhaja, Md Tausif Murshed, and Xingan David Kan. 2022. “Field Experiment of Mixed Traffic – Interaction between Adaptive Cruise Control (ACC) and Human Drivers.” In *Transportation Research Board 101st Annual Meeting*.

Gunter, George, Derek Gloudemans, Raphael E Stern, Sean McQuade, Rahul Bhadani, Matt Bunting, Maria Laura Delle Monache, Roman Lysecky, Benjamin Seibold, and Jonathan Sprinkle. 2020. “Are Commercially Implemented Adaptive Cruise Control Systems String Stable?” *IEEE Transactions on Intelligent Transportation Systems* 22 (11). IEEE: 6992–7003.

Gunter, George, Caroline Janssen, William Barbour, Raphael E Stern, and Daniel B Work. 2019. “Model-Based String Stability of Adaptive Cruise Control Systems Using Field Data.” *IEEE Transactions on Intelligent Vehicles* 5 (1). IEEE: 90–99.

He, Yinglong, Marcello Montanino, Konstantinos Mattas, Vincenzo Punzo, and Biagio Ciuffo. 2022. “Physics-Augmented Models to Simulate Commercial Adaptive Cruise Control (ACC) Systems.” *Transportation Research Part C: Emerging Technologies* 139. Elsevier: 103692.

Hung, Yun-Chu, and Kuilin Zhang. 2022. “Impact of Cooperative Adaptive Cruise Control on Traffic Stability.” *Transportation Research Record* 2676 (12). SAGE Publications Inc: 226–241. doi:10.1177/03611981221094822.

ITE. 2009. *Traffic Engineering Handbook, 6th Edition*. <https://trid.trb.org/view/887821>.

James, Rachel M, Christopher Melson, Jia Hu, and Joe Bared. 2019. “Characterizing the Impact of Production Adaptive Cruise Control on Traffic Flow: An Investigation.” *Transportmetrica B: Transport Dynamics* 7 (1). Taylor & Francis: 992–1012.

Knoop, Victor L, Meng Wang, Isabel Wilmink, D Marika Hoedemaeker, Mark Maaskant, and Evert-Jeen Van der Meer. 2019. “Platoon of SAE Level-2 Automated Vehicles on Public Roads: Setup, Traffic Interactions, and Stability.” *Transportation Research Record* 2673 (9). SAGE Publications Sage CA: Los Angeles, CA: 311–322.

Lapardhaja, Servet, Yaobang Gong, Md Tausif Murshed, and Xingan David Kan. 2021. “Impact of Commercially Available Automated Vehicles on Freeway Bottleneck Capacity.” In *Transportation Research Board 100th Annual Meeting*.

Li, Tienan, Danjue Chen, Hao Zhou, Jorge Laval, and Yuanchang Xie. 2021. “Car-Following Behavior Characteristics of Adaptive Cruise Control Vehicles Based on Empirical Experiments.” *Transportation Research Part B: Methodological* 147. Elsevier: 67–91.

Li, Tienan, Danjue Chen, Hao Zhou, Yuanchang Xie, and Jorge Laval. 2022. "Fundamental Diagrams of Commercial Adaptive Cruise Control: Worldwide Experimental Evidence." *Transportation Research Part C: Emerging Technologies* 134. Elsevier: 103458.

Liu, Hao, Xingan (David) Kan, Steven E. Shladover, Xiao-Yun Lu, and Robert E. Ferlis. 2018. "Modeling Impacts of Cooperative Adaptive Cruise Control on Mixed Traffic Flow in Multi-Lane Freeway Facilities." *Transportation Research Part C: Emerging Technologies* 95 (October): 261–279. doi:10.1016/j.trc.2018.07.027.

Liu, Hao, Xiao-Yun Lu, and Steven E. Shladover. 2019. "Traffic Signal Control by Leveraging Cooperative Adaptive Cruise Control (CACC) Vehicle Platooning Capabilities." *Transportation Research Part C: Emerging Technologies* 104 (July): 390–407. doi:10.1016/j.trc.2019.05.027.

Liu, Hao, Xiao-Yun Lu, and Steven E. Shladover. 2020. "Mobility and Energy Consumption Impacts of Cooperative Adaptive Cruise Control Vehicle Strings on Freeway Corridors." *Transportation Research Record* 2674 (9). SAGE Publications Inc: 111–123. doi:10.1177/0361198120926997.

Liu, Hao, Steven E. Shladover, Xiao-Yun Lu, and Xingan (David) Kan. 2021. "Freeway Vehicle Fuel Efficiency Improvement via Cooperative Adaptive Cruise Control." *Journal of Intelligent Transportation Systems* 25 (6). Taylor & Francis: 574–586. doi:10.1080/15472450.2020.1720673.

Makridis, Michail, Konstantinos Mattas, Aikaterini Anesiadou, and Biagio Ciuffo. 2021. "OpenACC. An Open Database of Car-Following Experiments to Study the Properties of Commercial ACC Systems." *Transportation Research Part C: Emerging Technologies* 125. Elsevier: 103047.

Makridis, Michail, Konstantinos Mattas, and Biagio Ciuffo. 2019. "Response Time and Time Headway of an Adaptive Cruise Control. An Empirical Characterization and Potential Impacts on Road Capacity." *IEEE Transactions on Intelligent Transportation Systems* 21 (4). IEEE: 1677–1686.

Mattas, Konstantinos, Michalis Makridis, Pauliana Hallac, María Alonso Raposo, Christian Thiel, Tomer Toledo, and Biagio Ciuffo. 2018. "Simulating Deployment of Connectivity and Automation on the Antwerp Ring Road." *IET Intelligent Transport Systems* 12 (9): 1036–1044. doi:10.1049/iet-its.2018.5287.

Milanés, Vicente, and Steven E Shladover. 2014. "Modeling Cooperative and Autonomous Adaptive Cruise Control Dynamic Responses Using Experimental Data." *Transportation Research Part C: Emerging Technologies* 48. Elsevier: 285–300.

Shang, Mingfeng, Benjamin Rosenblad, and Raphael Stern. 2022. "A Novel Asymmetric Car Following Model for Driver-Assist Enabled Vehicle Dynamics." *IEEE Transactions on Intelligent Transportation Systems* 23 (9). IEEE: 15696–15706.

Shang, Mingfeng, and Raphael E Stern. 2021. "Impacts of Commercially Available Adaptive Cruise Control Vehicles on Highway Stability and Throughput." *Transportation Research Part C: Emerging Technologies* 122. Elsevier: 102897.

Shi, Xiaowei, and Xiaopeng Li. 2021. "Constructing a Fundamental Diagram for Traffic Flow with Automated Vehicles: Methodology and Demonstration." *Transportation Research Part B: Methodological* 150. Elsevier: 279–292.

Shladover, Steven E., Dongyan Su, and Xiao-Yun Lu. 2012. "Impacts of Cooperative Adaptive Cruise Control on Freeway Traffic Flow." *Transportation Research Record* 2324 (1). SAGE Publications Inc: 63–70. doi:10.3141/2324-08.

Vander Werf, Joel, Steven E Shladover, Mark A Miller, and Natalia Kourjanskaia. 2002. "Effects of Adaptive Cruise Control Systems on Highway Traffic Flow Capacity." *Transportation Research Record* 1800 (1). SAGE Publications Sage CA: Los Angeles, CA: 78–84.

Wang, Hao, Yanyan Qin, Wei Wang, and Jun Chen. 2019. "Stability of CACC-Manual Heterogeneous Vehicular Flow with Partial CACC Performance Degrading." *Transportmetrica B: Transport Dynamics* 7 (1). Taylor & Francis: 788–813. doi:10.1080/21680566.2018.1517058.

Wang, M., S. P. Hoogendoorn, W. Daamen, B. van Arem, B. Shyrokau, and R. Happee. 2018. "Delay-Compensating Strategy to Enhance String Stability of Adaptive Cruise Controlled Vehicles." *Transportmetrica B: Transport Dynamics* 6 (3). Taylor & Francis: 211–229. doi:10.1080/21680566.2016.1266973.

Wang, Wenzuan, and Bing Wu. 2023. "The Fundamental Diagram of Mixed-Traffic Flow with CACC Vehicles and Human-Driven Vehicles." *Journal of Transportation Engineering, Part A: Systems* 149 (1). American Society of Civil Engineers: 04022116.

Yang, Mingyuan, Xingan David Kan, and Kemal Ulas Yagantekin. 2023. "Modeling Car-Following Behaviors of Adaptive Cruise Control-Equipped Vehicles Under Heterogeneous Desired Speeds." In *Transportation Research Board 102nd Annual Meeting*.

Yang, Mingyuan, Servet Lapardhaja, Pablo Chon Kan, Xingan David Kan, Hao Liu, and Xiao-Yun Lu. 2022. "Modeling CAV Car Following on Freeways and Arterials—Case Study of Adaptive Cruise Control (ACC) Equipped Vehicles." In *Transportation Research Board 101st Annual Meeting*.

Yu, Weijie, Xuedong Hua, and Wei Wang. 2023. "Stability and Capacity for Heterogeneous Traffic Flow Mixed with Vehicles in Multiple Controls." *Transportmetrica B: Transport Dynamics* 11 (1). Taylor & Francis: 649–682. doi:10.1080/21680566.2022.2113476.

Zare, Arian, Mingfeng Shang, Xingan David Kan, and Raphael Stern. 2023. "Modeling Car-Following Behavior of Electric Adaptive Cruise Control Vehicles Using Experimental Testbed Data." In *26th IEEE International Conference on Intelligent Transportation Systems ITSC 2023*.

Appendix

The data from the field experiments are organized in folders with the setup presented in Figure 13. For instance, a trial with Long gap setting, +0 desired speed, free flow speed of 72 km/hr (45 mph) and speed fluctuation down to 24 km/hr (15 mph) will be found in the path "Long\0_desired\45\15"

[Figure 13 here]

The data consists of Time (s), the speed (km/h) of the following vehicle, the speed (km/h) of the leading vehicle, the speed (km/h) of the following vehicle with a smoothing algorithm applied,

the speed (km/h) of the leading vehicle with a smoothing algorithm applied, and the spacing (m) between the leading and the following vehicle.

Tables

Table 1 Combinations of initial and terminal field test speeds.

Table 2 Steady-state minimum headways of ACC-equipped EVs.

Table 3 Headway change for various desired speeds.

Table 1 Combinations of initial and terminal field test speeds.

Initial free-flow speed (km/hr)	Terminal reduced speeds (km/hr)
96	72, 56, 40, 24, 0
88	72, 56, 40, 24, 0
72	56, 40, 24, 0
56	40, 24, 0

Table 2 Steady-state minimum headways of ACC-equipped EVs.

Free Flow Speed: 96 km/hr				
	ACC Gap Selection			
	Short	Medium	Long	Extra Long
Minimum headway (s)	1.23	1.50	1.77	2.30
Time Gap (s)	1.06	1.33	1.60	2.13
Free Flow Speed: 88 km/hr				
	ACC Gap Selection			
	Short	Medium	Long	Extra Long
Minimum headway (s)	1.27	1.6	1.84	2.35
Time Gap (s)	1.08	1.41	1.65	2.16
Free Flow Speed: 72 km/hr				
	ACC Gap Selection			
	Short	Medium	Long	Extra Long
Minimum headway (s)	1.40	1.69	1.92	2.41
Time Gap (s)	1.17	1.46	1.69	2.18
Free Flow Speed: 56 km/hr				
	ACC Gap Selection			
	Short	Medium	Long	Extra Long
Minimum headway (s)	1.44	1.73	1.96	2.25
Time Gap (s)	1.14	1.43	1.66	1.95

Table 3 Headway change for various desired speeds.

Gap Setting	Desired Speed (unit: km/hr)	Headway Change (Std, unit: seconds)
Short	0	0.074 (0.090)
	8	0.033 (0.052)
	16	0.013 (0.042)
Medium	0	0.090 (0.075)
	8	0.002 (0.076)
	16	0.021 (0.067)
Long	0	0.058 (0.058)
	8	0.037 (0.041)
	16	0.021 (0.042)
Extra Long	0	0.029 (0.061)
	8	-0.005 (0.025)
	16	0.020 (0.046)

Figures

Figure 1 Torque and power vs. engine speed for ICE (left) vs. EVs (right).

Figure 2 Initial stabilization process.

Figure 3 Example speed profile of field test.

Figure 4 Distribution of minimum steady-state headways of ACC-equipped Hyundai IONIQ

Figure 5 Hyundai IONIQ 5 time-space diagram: 88 to 40 to 88 km/hr, short gap, same desired speeds.

Figure 6 Toyota Corolla time-space diagram: 88 to 40 to 88 km/hr, short gap, same desired speeds.

Figure 7 Hyundai IONIQ 5 time-space diagram: 88 to 40 to 88 km/hr, short gap, +8 km/hr desired speed.

Figure 8 Toyota Corolla time-space diagram: 88 to 40 to 88 km/hr, short gap, +8 km/hr desired speed.

Figure 9 Polestar time-space diagram: 88 to 40 to 88 km/hr, short gap, same desired speeds.

Figure 10 Tesla time-space diagram: 88 to 40 to 88 km/hr, short gap, same desired speeds.

Figure 11 Tesla time-space diagram: 88 to 40 to 88 km/hr, short gap, +8 km/hr desired speed.

Figure 12 IONIQ 5 and Tesla acceleration and deceleration rates distributions.

Figure 13 Field data folder organization.

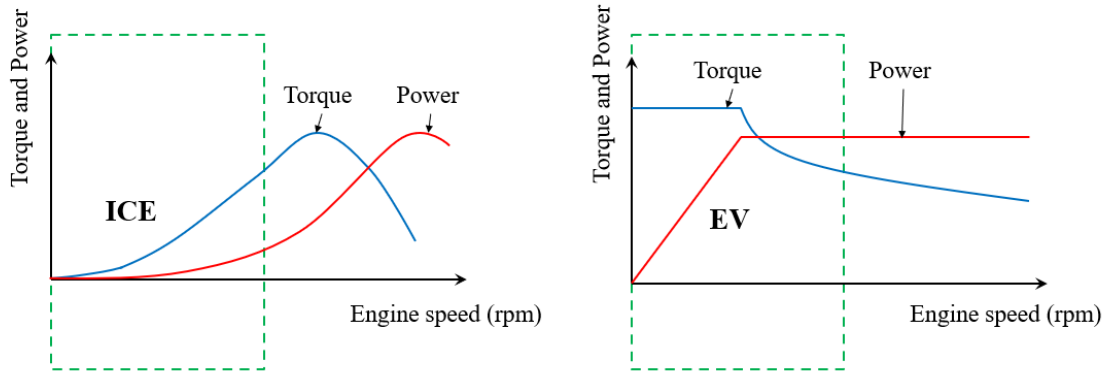


Figure 1 Torque and power vs. engine speed for ICE (left) vs. EVs (right).

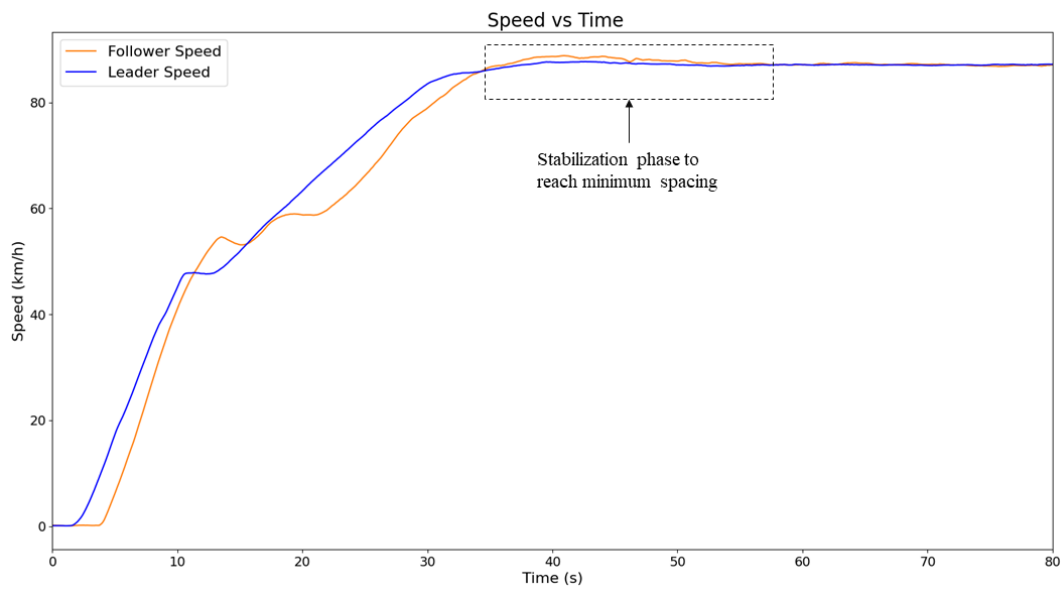


Figure 2 Initial stabilization process.

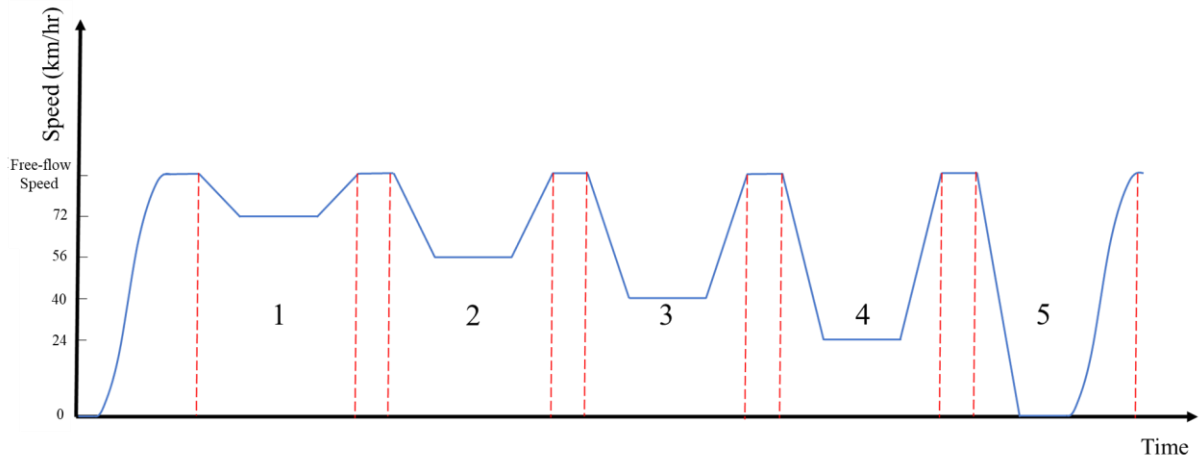


Figure 3 Example speed profile of field test.

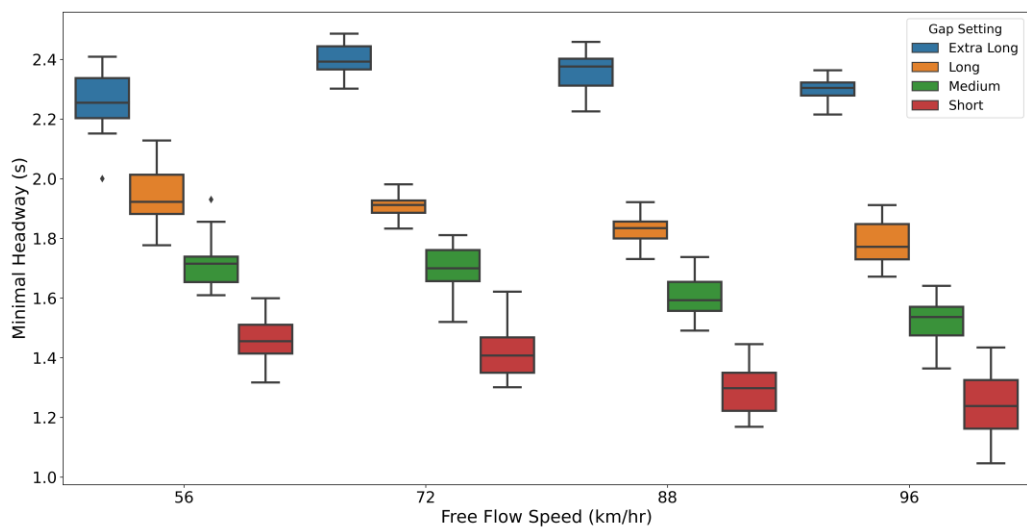


Figure 4 Distribution of minimum steady-state headways of ACC-equipped Hyundai IONIQ 5.

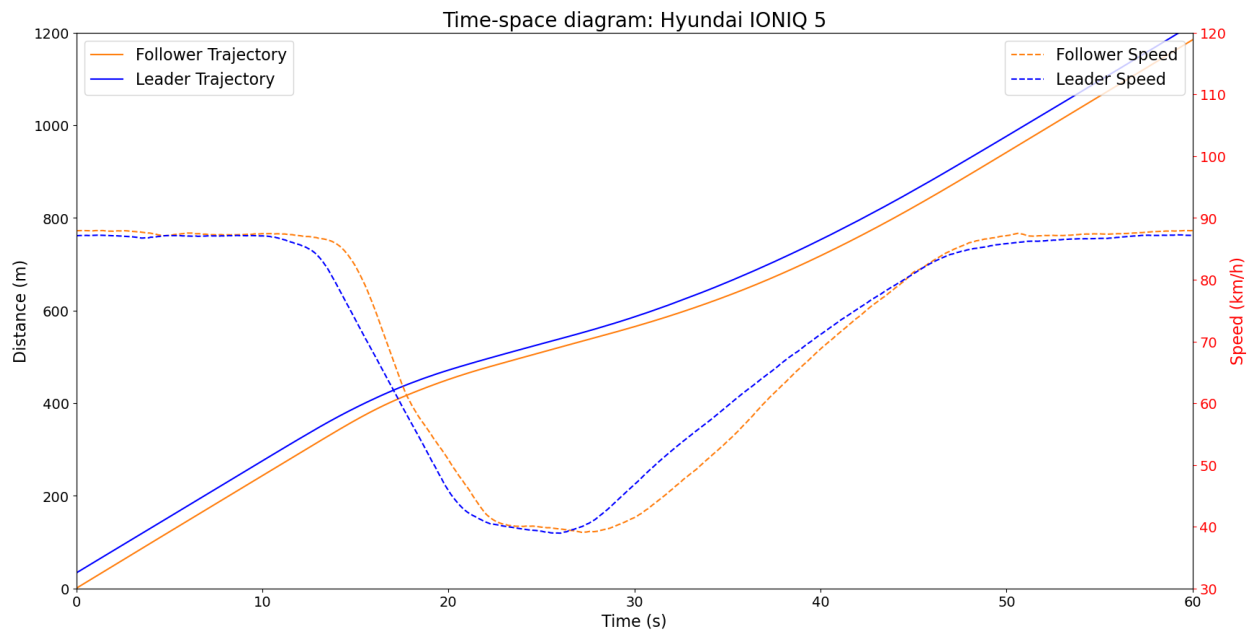


Figure 5 Hyundai IONIQ 5 time-space diagram: 88 to 40 to 88 km/hr, short gap, same desired speeds.

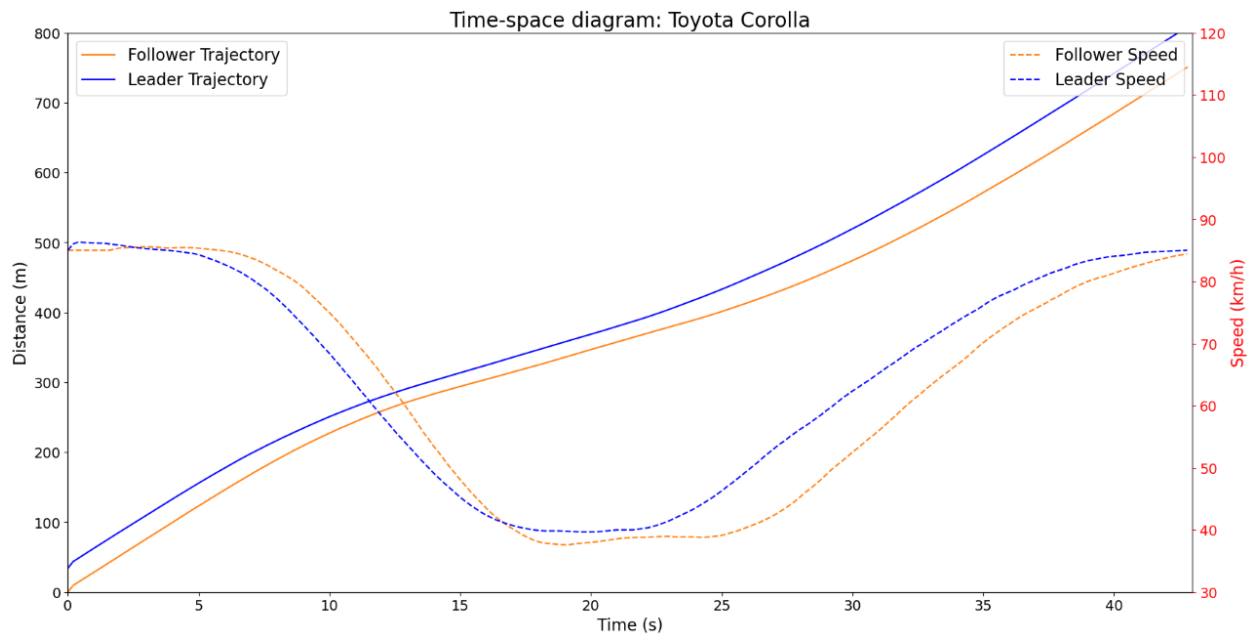


Figure 6 Toyota Corolla time-space diagram: 88 to 40 to 88 km/hr, short gap, same desired speeds.

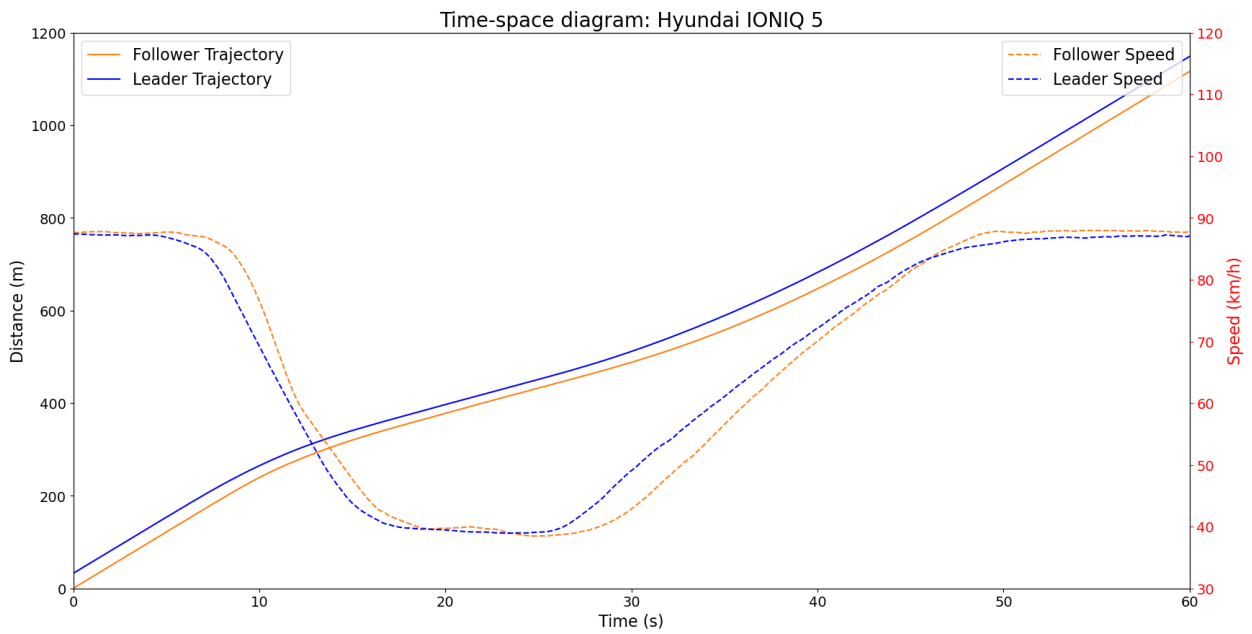


Figure 7 Hyundai IONIQ 5 time-space diagram: 88 to 40 to 88 km/hr, short gap, +8 km/hr desired speed.

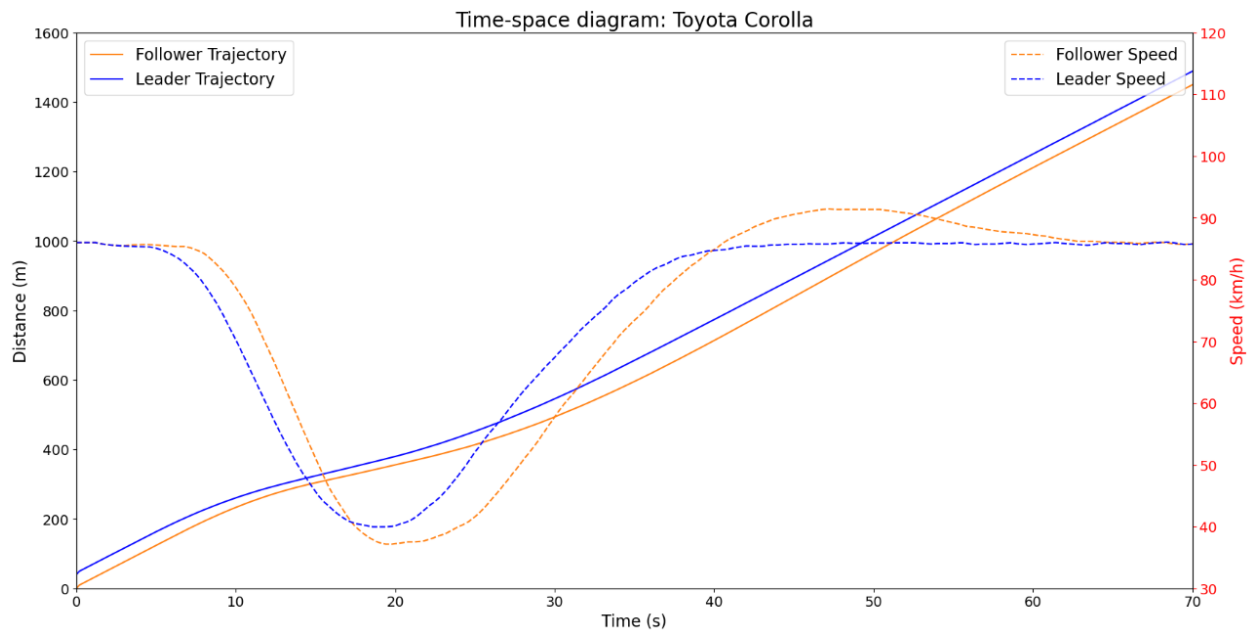


Figure 8 Toyota Corolla time-space diagram: 88 to 40 to 88 km/hr, short gap, +8 km/hr desired speed.

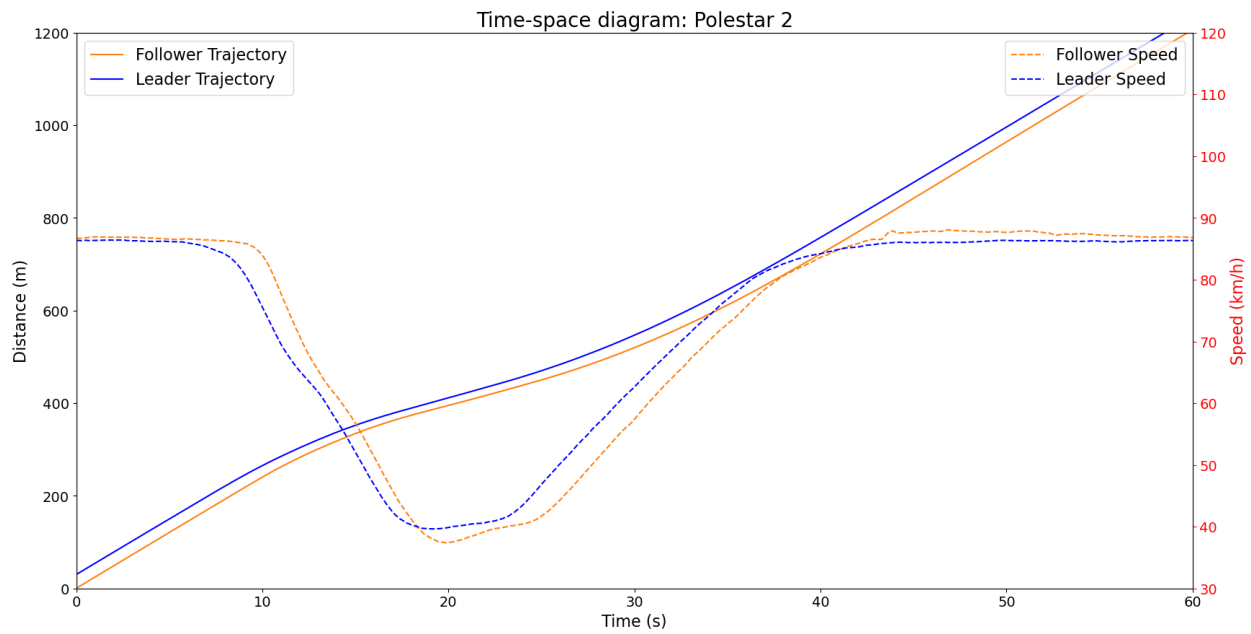


Figure 9 Polestar time-space diagram: 88 to 40 to 88 km/hr, short gap, same desired speeds.

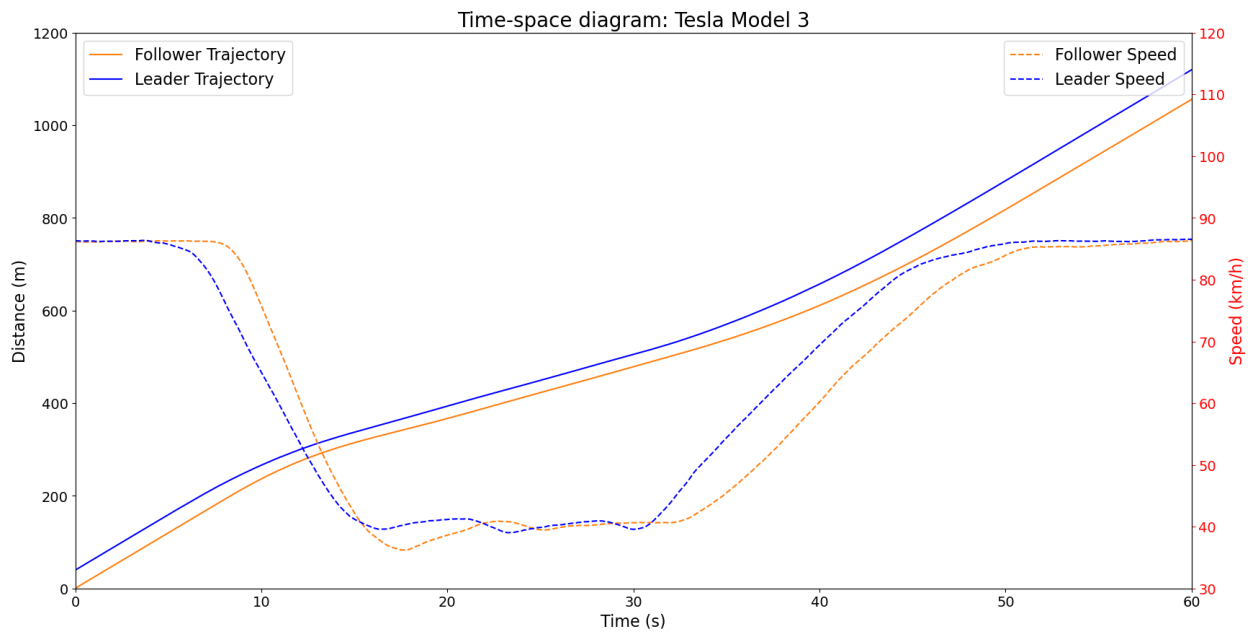


Figure 10 Tesla time-space diagram: 88 to 40 to 88 km/hr, short gap, same desired speeds.

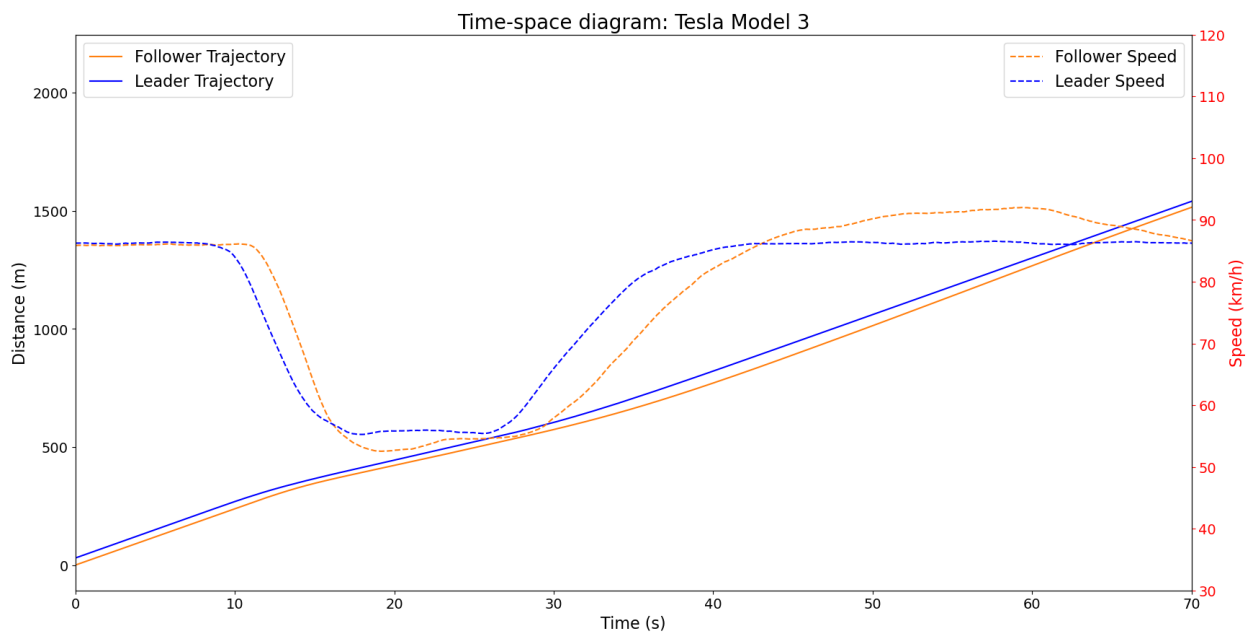


Figure 11 Tesla time-space diagram: 88 to 40 to 88 km/hr, short gap, +8 km/hr desired speed.

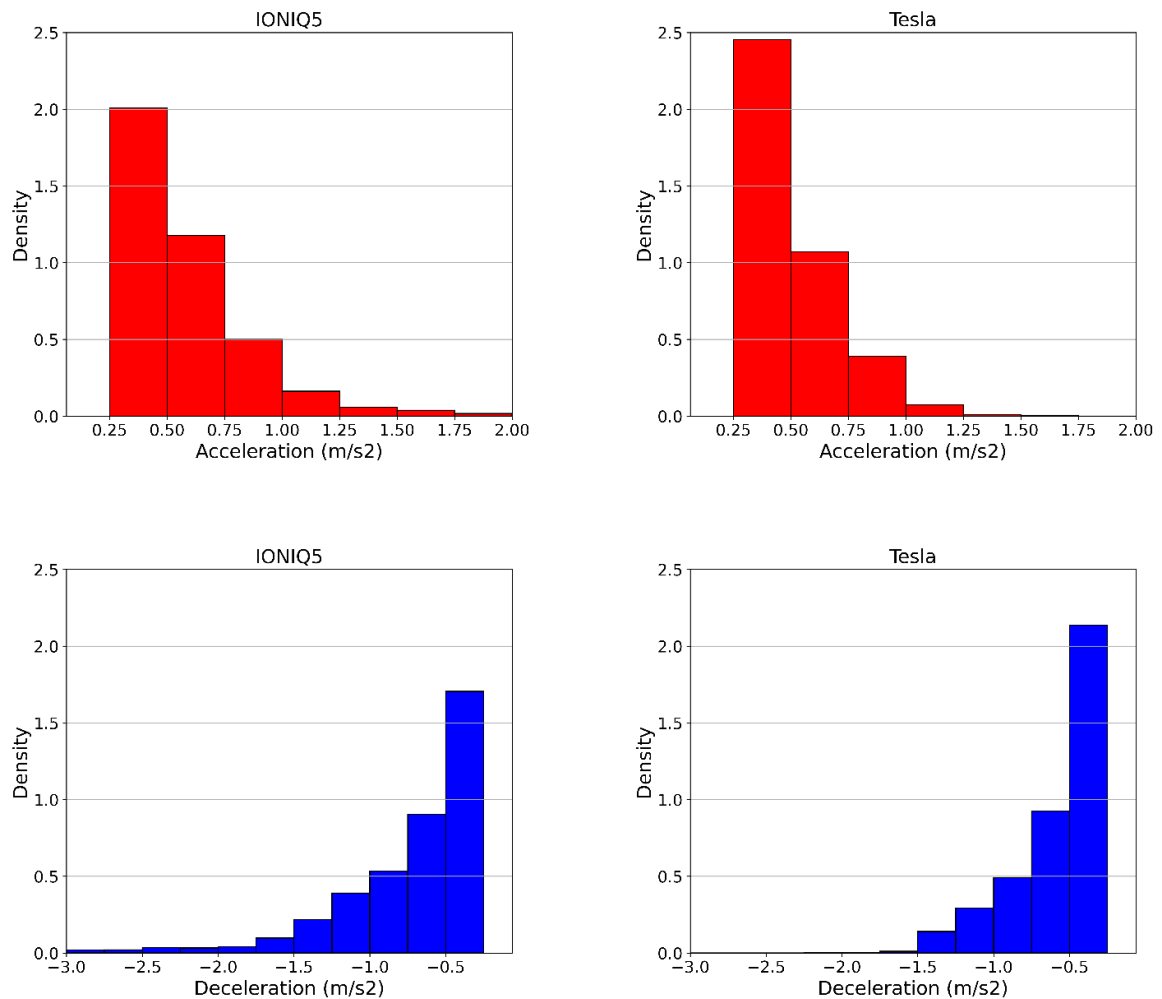


Figure 12 IONIQ 5 and Tesla acceleration and deceleration rates distributions.

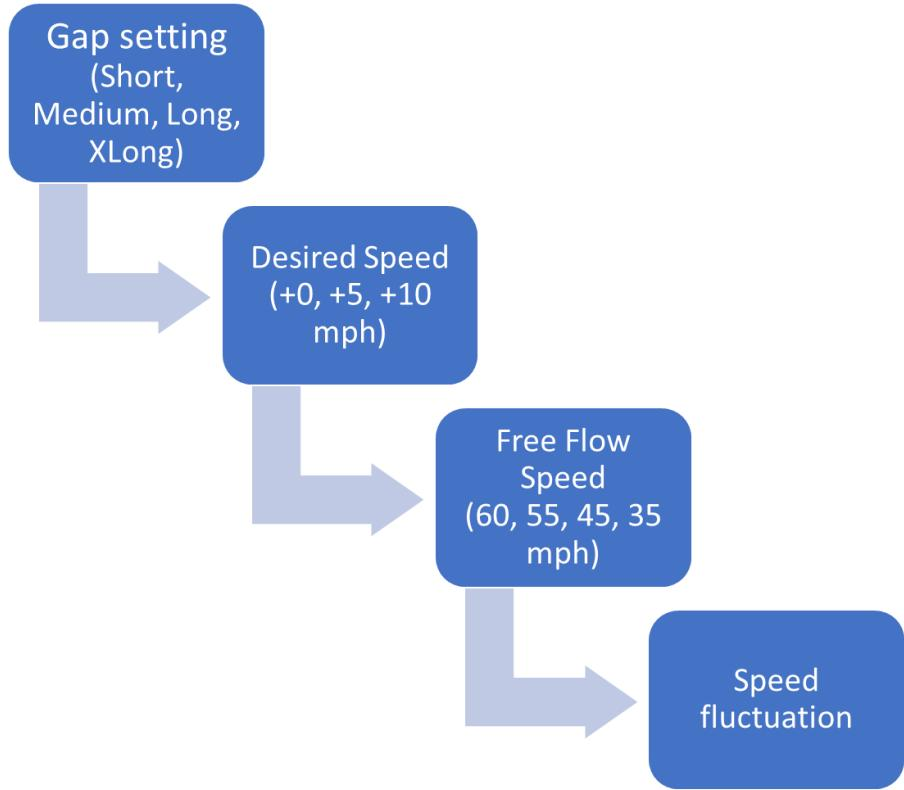


Figure 13 Field data folder organization.